

Multilinear analysis of the systematics of proton radioactivity

Mário B. Amaro , Daniel Karlsson, and Chong Qi 

Department of Physics, KTH Royal Institute of Technology, AlbaNova University Center, SE-10691 Stockholm, Sweden



(Received 11 June 2023; accepted 6 November 2023; published 20 November 2023)

It is shown that the proton formation probabilities, extracted from experimental decay half-lives, can be well reproduced by a simple multilinear formula with only three parameters. The parameters obtained by considering the standard root mean square deviation and the mini-max criteria are very similar to each other. In addition, we applied Bayesian analysis to study the uncertainties of the parameters and the model predictions. In this way we explain the systematics of proton decay half-lives. The multilinearity of the model also provides a way to classify the relative hindrance of different proton decays. All the recent experimental data agree very well with the model prediction. Our Bayesian analysis suggests that those new data do help constrain the uncertainty of the model parameters.

DOI: [10.1103/PhysRevC.108.054311](https://doi.org/10.1103/PhysRevC.108.054311)

I. INTRODUCTION

Significant recent advances have been made in studying the nuclear proton radioactivity [1–5]. In total there are now nearly 50 observed proton decay events from the ground and low-lying isomeric states of neutron-deficient nuclei above ^{100}Sn . In the systematic studies of nuclear radioactivity, there exists a striking linear correlation between the logarithm of the alpha decay half-life and the energy of the outgoing α particle. This is known as the Geiger-Nuttall law [6] which works extremely well even today in describing α as well as heavier cluster decays [7,8]. Theoretically, one would expect the proton radioactivity to follow a similar behavior since the process, as in α decay, is dominated by the tunneling through the Coulomb and centrifugal barriers. However, there has been no success in finding a simple linear pattern in proton decay half-life systematics [9–12]. Instead, the then available proton decay data seem to cluster around roughly two straight lines with large spread. In addition, there are quite a few data falling in between the two lines. That makes it difficult not only for having a reliable systematic prediction on the decay half-life but also for understanding the physics behind the decay process.

The proton decay is often described as the tunneling of a simple (unbound) proton single-particle orbital. In reality that may not always be true since the wave functions of both the initial and final states of the decay can be of complex many-body nature. Therefore the decay rate can be affected by the overlap between the initial, final and decaying proton wave

functions in addition to the tunneling rate. The overlap can be evaluated through the so-called decay formation amplitude within the two-step R -matrix approach. The half-life can be evaluated accordingly as [7]

$$T_{1/2} = \frac{\ln 2}{\nu} \left| \frac{H_l^+(\chi, \rho)}{RF_l(R)} \right|^2, \quad (1)$$

where F_l is the formation amplitude and $H_l^+(\chi, \rho)$ is the Coulomb-Hankel function with standard arguments. ν and l are the velocity and angular momentum of the emitted proton, respectively. R is the radius where the F_l and H_l functions match, which can be taken as the touching point. Both functions F_l and H_l depend on R but their ratio does not. In the extreme single-particle model, the proton formation amplitude can be simply expressed as

$$F(R) = \frac{1}{R^{3/2}}, \quad (2)$$

which defines the so-called particle decay unit (pdu) [13]. The deviations of the proton decay formation amplitude from the pdu value would therefore reflect the influence of nuclear structure effect on the decay. On the first glance, one may deem every proton decay case to be different as they connect different and complex initial and final states and therefore would not expect any regular systematic behavior. However, as we understand now and will illustrate later, the dominant nuclear structure effects for proton decay are actually the nuclear deformation and pairing correlation, both of which mostly show very smooth behavior when going from one nucleus to neighboring ones. Therefore, it can still be interesting to search for regular behaviors in the proton decay systematics, even if it may not be as simple as the Geiger-Nuttall law. The possible existence of such regular pattern could help reveal the fundamental mechanism underlying the decay and the structure of the many-body states involved. From a general perspective, one can state that one of the most important aspects in nuclear and many-body physics is the emergence

*chongq@kth.se

Published by the American Physical Society under the terms of the [Creative Commons Attribution 4.0 International](https://creativecommons.org/licenses/by/4.0/) license. Further distribution of this work must maintain attribution to the author(s) and the published article's title, journal citation, and DOI. Funded by [Bibsam](https://www.bibsam.se/).

of regular and simple patterns from the complex correlation, without which it would be very difficult even to solve the many-body wave function.

In this work we will focus on studying the systematic properties of the formation amplitude instead of the half-life since the Coulomb-Hankel function can be calculated analytically and is independent of the nuclear interaction [11]. The experimental formation amplitude, which reflects the nuclear structure effect on the decay, can be extracted when the experimental decay half-life and Q value are known [14,15]. We will show that all available proton formation amplitudes (and equivalently the decay half-lives) including the most recent data [1–5] can be described extremely well by a simple multilinear model with only three parameters. The uncertainty of the model prediction will also be evaluated based on variance analysis and Bayesian analysis.

II. THE MODEL

We assume that the proton formation amplitude data can be described by a system of multiple lines as

$$y_k = (k - 1)(\alpha x + \beta) + o \quad (3)$$

with the same basic parameters α (slope), β (intercept), and o (offset). The difference between them lying in an integer proportionality k . Each datum is thus associated with a classifier k which can take values between $k = 1$ and N , where N is the maximum number of lines to be considered in the system. We would like to keep the model as simple as possible. For that one aims to find the minimal value of N that can describe well the available data. In practice we choose to study two y_k quantities, the logarithm of $|RF_l(R)|^2$ (in unit fm^{-1}) and $F_l(R)R^{3/2}$ (unitless), which will be referred to as the proton decay formation probability and the formation amplitude in particle decay unit, respectively. We study their evolution as a function of the quantity $x = \rho' = \sqrt{AZ_d(A_d^{1/3} + 1)}$ with $A = 1/(A_d + 1)$.

The formula Eq. (3) is proposed by first considering the fact that the logarithm of the half-life and the Coulomb-Hankel function are also proportional to ρ' [11]. And there should be no systematic dependence of the formation probability on the decay Q value (or χ). In addition, as indicated in Eq. (2), the formation probability should decrease in the extreme single-particle picture. In that case we would expect α to be negative since the formation amplitude decreases as increasing R (or ρ'). The parameter o would be a small number representing the minimum value of the predicted formation amplitude in the large R limit or for the least favored proton decay classification with $k = 1$. Correspondingly, $k = N$ classifies the most favored proton decay events. There will be only one line with $k = N = 2$ in the ideal case where the formation probability varies smoothly as predicted by the single-particle model.

A. Determination of the model parameters

To determine the three parameters of the multilinear model, we first consider to minimize the standard root mean square

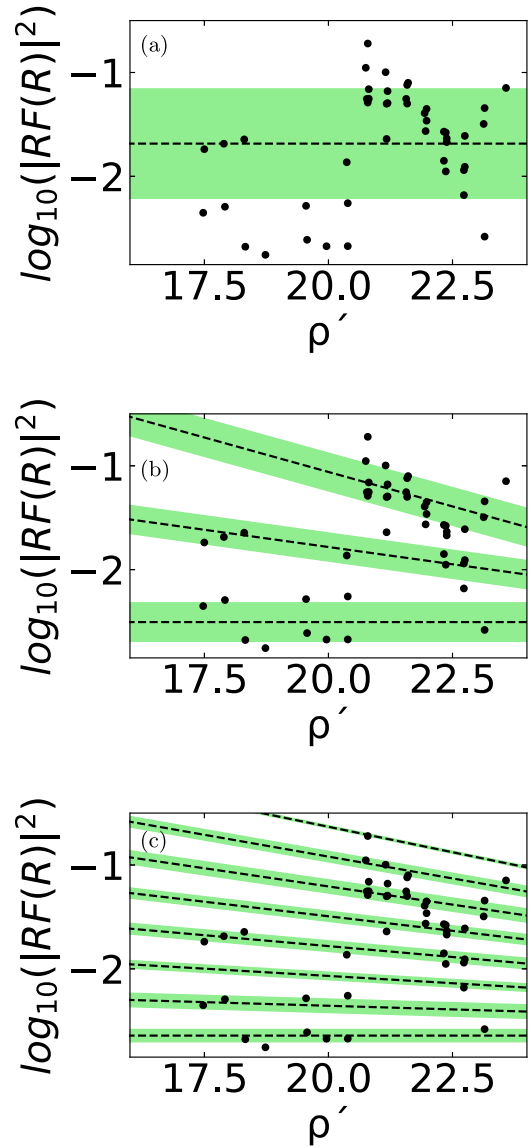


FIG. 1. Comparison between logarithm experimental proton decay formation probabilities (in unit fm^{-1}) and the multilinear model with $N = 1$ (a), 3 (b), and 8 (c). The shaded area marks the 1σ deviation from the mean value of the fit.

deviation (RMSD) as

$$\sigma^2 = \frac{1}{T} \sum_{i=1}^T (y_i - y_{k_i})^2, \quad (4)$$

where y_i is the i th observed value up to T and y_{k_i} is the corresponding predicted value with classifier k determined by taking the k th line that is closest to the data point. In practice, for a given N , we search for the global minimum of σ on a dense grid defined in the (α, β, o) space. For each set of α, β , and o , we first assign a classifier k for each data point and then sum over the square deviations. The set that gives the minimal σ value is returned as the optimal parameters.

In Fig. 1 we compared the proton decay formation probabilities extracted from experimental decay half-lives and the

multilinear fits with $N = 1, 3$, and 8 . The rest of the results are given in the Supplemental Material [16]. As expected and can be inferred based on earlier studies (c.f., Fig. 2 in Ref. [11]), the experimental data are far from being explainable by a linear fit or fitting to two lines. However, a very stimulating result as one can see from Fig. 1 is that a good agreement between data and the multilinear fit can be achieved already with $N = 3$. With $N = 3$ and only three parameters, one gets a much better description than earlier two-line analyses with four (or more) parameters.

One can expect the RMSD values from above least squares method to decrease as increasing N . However, this is an uninteresting result in relation to the risk that uncertainty of a model may increase as well, in particular for complex nonlinear models. In Fig. 1 we also plotted the evolution of the variance σ^2 as a function of N . In addition to that, we analyzed a product $\sigma^2 N^2$ which may to some extent illustrate the total uncertainty of the model, where one sees a big drop at $N = 3$ and, inconsistent with what we speculated above, start to increase for $N > 8$. We therefore deem our $N = 3$ model as the simplest model with reliable predictions while the $N = 8$ model as the most optimal model with lowest variance and uncertainty. The optimal parameters were found to be $[\alpha, \beta, o] = [-0.01400, 0.56727, -2.64286]$ for $N = 8$. Those correspond to a variance of about $\sigma^2 = 0.00317$ for all observed data. As a comparison, for $N = 3(2)$ one reaches $\sigma^2 = 0.02975 (0.07914)$, which indicates that the experimental data can be reproduced within a factor of around 1.5 (2).

We have also compared the results from fitting with and without the five new or updated data. The results are quite similar to each other. No noticeable increase in σ is observed.

In Fig. 2 we plotted the differences between the experimental and theoretical proton decay formation probabilities together with the experimental errors and theoretical uncertainty. For $N = 8$ the differences are close to zero and are significantly smaller than many of the experimental error bars. For $N = 3$, there is still one datum that deviates quite noticeably from the systematics. That corresponds to the $l = 5$ decay from the presumed ^{146}Tm isomeric state. We have also studied the statistical distributions of the differences which follow nicely the Gaussian distribution around mean value zero for all N values we studied.

We focus on minimizing the RMSD, Rq. (4), for the above and following analyses. Another common criterion is to minimize the mean squared weighted deviation

$$\chi^2 = \sum_{i=1}^T \frac{(y_i - y_{k_i})^2}{\sigma_i^2}, \quad (5)$$

where σ_i denotes the error in the corresponding experimental data as shown in Fig. 2. The results are quite similar to what we got above. Part of the results are given in the Supplemental Material [16].

In addition to the least squares method above, the so-called mini-max method was applied in nuclear physics in Refs. [17–19] and is getting very popular nowadays in various artificial intelligence algorithm studies. We are interested in that method in particular by considering the relatively large discrepancy seen in the $N = 3$ model in Fig. 2. The object

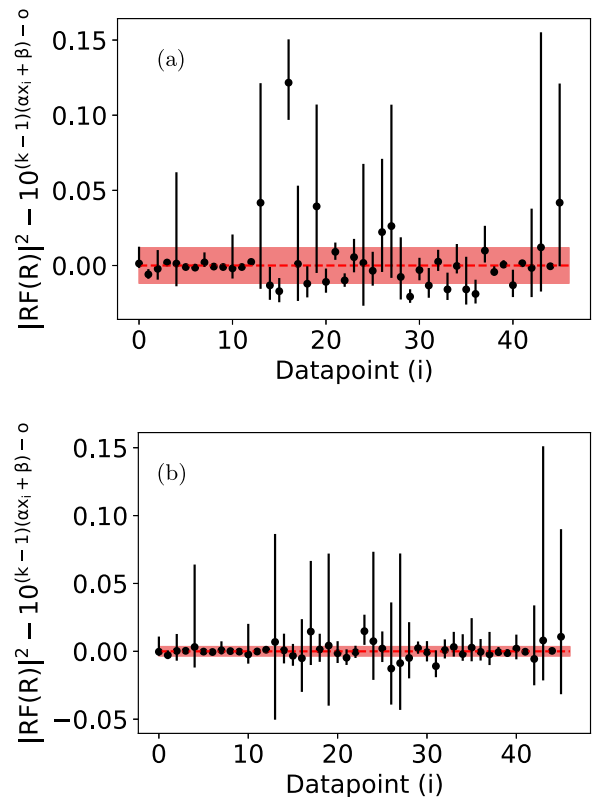


FIG. 2. The deviations of experimental proton decay formation probabilities (in unit fm^{-1} , without logarithm) from the multilinear fits with $N = 3$ (a) and 8 (b). The shaded area marks the theoretical uncertainty. The bar indicates the error in the experimental formation probabilities that are extracted based on the errors in the experimental decay half-lives and Q values.

of the mini-max fit is to minimize the maximum deviation or the largest discrepancy in the parameter and data space (α, β, o, i) as

$$\varepsilon = \arg \min_{\hat{\alpha}} \max_i |y_i - y_{k_i}|, \quad (6)$$

where $\arg \min$ ($\arg \max$) stands for the argument for which the value of the given expression attains its minimum (maximum) value and $\hat{\alpha}$ denote the set of parameters (α, β, o) . We adapted a procedure that is similar to the above least squares method. On each grid point of the parameter space, the proton decay event(s) with the largest deviation is returned. Then one can search for the parameter set that minimizes that value. After the optimal $\hat{\alpha}$ is determined, there will be four data points (number of parameters plus one) with the same largest deviation value. In other words, the parameters are determined by just very few data points with the largest deviation. If those points deviate strongly from the systematic behavior of the rest data points, one would observe a large difference between the fits from above least squares and mini-max methods. On the contrary, the parameters thus determined tend to be pretty similar to those given by the least squares method. Therefore we only plotted the $N = 3$ model in Fig. 3 as a comparison. In that case a noticeable difference is seen in the slope values from the mini-max and least squares methods but is within

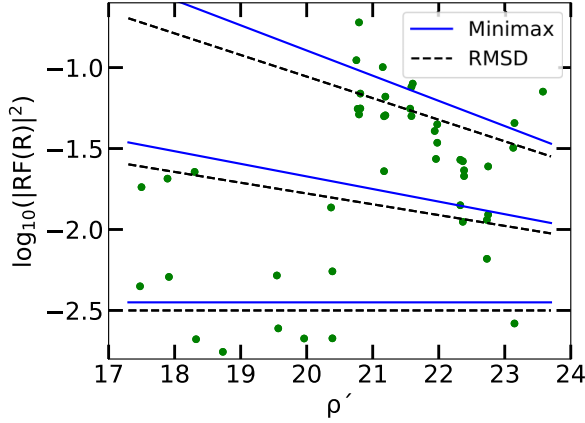


FIG. 3. Comparison between logarithm of experimental proton decay formation probabilities (in unit fm^{-1}) and the multilinear model with $N = 3$ with parameters optimized with the mini-max approach (solid) and the least squares method (dashed) from Fig. 1.

the theoretical uncertainty. Detailed results can be found in the Supplemental Material [16]. The similarity between the least square and the mini-max fit indicate that the present model analysis is quite robust and does catch the systematic behaviors of all data.

B. The Bayesian analysis

The third method we consider to constrain the model parameters is the Bayesian statistical analysis which can be in particular useful when the number of data points is small. There is increasing interest in applying Bayesian analysis in various theoretical nuclear physics studies (see, for example, Refs. [20,21]) in connection, in particular, to the increasing emphasis on quantifying the uncertainties of theoretical models. The Bayesian analysis adapts a philosophy which is quite different from the standard fitting procedures as we have done above. Instead of looking for the optimal parameters and predicted values, Bayesian analysis aims at constraining the distributions/uncertainties of the parameters as well as the predictions. We only explain it briefly here based on how we have implemented it for our multilinear analysis. The Bayesian analysis is based on the theorem that

$$\text{posterior} \propto \text{prior} \times \text{likelihood}, \quad (7)$$

where the prior distribution represents our initial or present knowledge of the parameters and the likelihood distribution evaluates the probability the chosen parameters in describing the observed data. The likelihood is assumed to be

$$\text{likelihood} = \prod_i \frac{1}{\sqrt{2\pi}\sigma^2} e^{-\frac{(y_i - \hat{y}_i)^2}{2\sigma^2}}. \quad (8)$$

The posterior thus obtained from the product, after normalization, gives us an updated knowledge on the parameters. The initial prior can be taken as Gaussian or uniform distributions. It is hoped that a good constraint on the parameters can be obtained independent of the initial choice with increasing number of data points. That is indeed the case as we saw from the Bayesian analysis of the proton decay data by gradually

increasing the number of data points included in the analysis. The results for both the parameters and the predicted values got quite close to those from the least squares method when the majority of the data are taken into account. In particular, when the most recent data from Refs. [1–5] are taken into account, one notices a quite large decrease in the theoretical uncertainty in the distribution of the parameters.

Part of the results we obtained from the Bayesian analysis are plotted in Fig. 4. The results for both the theoretical uncertainty/width of the distributions as well as their mean values are quite close to those obtained from the least squares method. The mean values of the parameters are also very close to those from the least squares method, which are nearly identical for $N = 3$ and a bit separated for $N = 8$ but within the theoretical uncertainty. Another remarkable feature is that the distribution of the slope parameter α and the intercepts $\beta + o$ are dominated by a small area of the parameter space and follows a linear pattern.

III. DISCUSSION

Unlike proton decay, α decay systematics can be rather well described by the original Geiger-Nuttall law and its various generalizations [6,7,22]. One main reason for the good agreement is the smooth transition in the nuclear structure and pairing correlations, which dominate the α formation process, when going from one nucleus to its neighboring nuclei. On the contrary, the proton decay formation probability can be rather sensitive to the nuclear deformation, where the decay is from a small spherical component of the deformed state. The formation probability can also be sensitive to the pairing correlation (but in a way that can be opposite to α decay) as well as the neutron-proton residual correlation/coupling [2]. From a simple theoretical perspective, the proton emitter can be described by the coupling of the outgoing proton and the daughter core. The deformed single-particle orbital (denoted by Nilsson quantum number Ω) of the outgoing proton can be expanded in its spherical components as

$$\Psi(\Omega) = \sum_{njl} c_{njl}^{\Omega} |njl\rangle. \quad (9)$$

In that case the corresponding formation amplitude would be proportional to

$$F_i^{\Omega}(R) \propto u_{ji}^{\Omega} c_{jl}^{\Omega} \frac{1}{R^{3/2}}, \quad (10)$$

where we assume the single particle states are the same as in the p.d.u. formalism and l denotes the decaying proton orbital and u is the probability that the orbital is empty in the daughter nucleus after the decay.

In a well-deformed nucleus the decay can proceed through both the small and large components of the spherical components of the deformed orbit (see, for example, Fig. 6 in Ref. [8]). Both scenarios have been observed experimentally. In spherical or weakly deformed nuclei the decay proceeds through the only component that is available and, as a result, the formation probability is large and can approach unity when expressed in the particle decay unit. The pairing

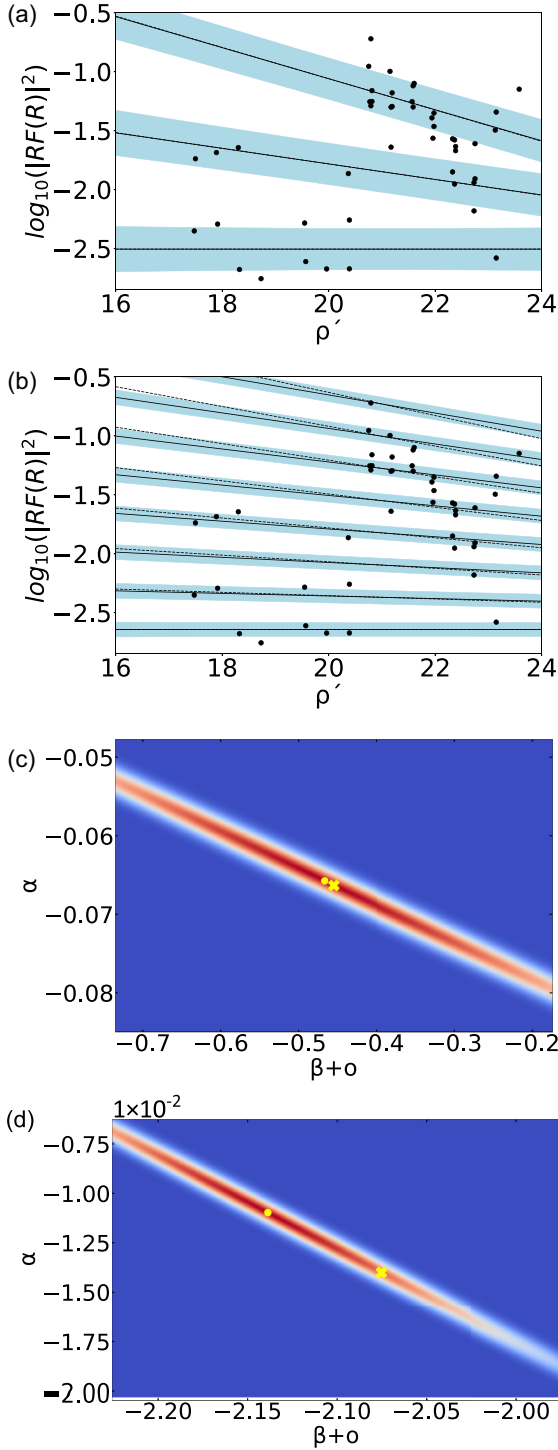


FIG. 4. Comparison between logarithm of experimental proton decay formation probabilities (in unit fm^{-1}) and the multilinear model with $N = 3$ (a) and 8 (b). The distributions of the parameters in the lower panels (c) and (d) of the figure, plotted as α versus $\beta + o$ for simplicity, is determined by the Bayesian analysis. The shaded area is the distribution of the predicted values from those parameter distributions. Their mean values are indicated by the solid lines. The results from the least squares method are drawn as dashed lines for comparison which is indistinguishable for $N = 3$. The dots in the lower two panels mark the peak of the distribution while the cross are results from RMSD in Fig. 1.

correlation can play a tricky role in proton decay. The formation probability can actually be strongly suppressed if the decaying orbit is highly occupied in the remaining daughter nucleus due to interference from the pairing [leading to small u value in Eq. (10)].

One may have doubted whether the proton decay systematics would follow any correlation behavior at all. In Refs. [9–12], the proton decay data were roughly divided into two regions separated by mass number $A = 144$. The nuclei in the lighter mass region are mostly deformed. Therefore the division was often discussed in terms of nuclear deformation effects. But quite many proton emitters above $A = 144$ including the recent ^{149}Lu [3] are also expected to be deformed. In addition, there are quite a few cases in that heavier mass region that, in contrary to the rest, show strong hindrance in proton formation as in the lighter mass region. Our present multilinear model not only reproduce the available data including the most recent ones with high accuracy and precision but also indicates a much stronger correlation and systematic trend than those of the two region division. It may be interesting to mention that, with only three parameters, one can reach a mean deviation that is comparable to our complex and nonlinear artificial neural network analysis of the α and proton decay formation probabilities [23]. One can state that the regular multilinear behaviors we have found is a reflect on the smooth transition of the nuclear deformation and pairing correlations for most regions of proton decaying nuclei of interest. Otherwise, the extracted formation probabilities would have scattered around the whole phase space of $(\log_{10} |RF(R)|^2, \rho')$.

Among the still limited amount of observed data on proton decays, we have ten strongly hindered cases with $\log_{10} |RF(R)|^2 \sim -2.5$ which include most nuclei with $Z \leq 63$ (decay of small components of the deformed proton orbital) and the heavier ^{177m}Tl (decay of a hole state with vanishing u). There are nine cases show intermediate values. The rest 27 cases are strongly favored with formation amplitude closes to unity in pdu since decays involve either dominant component of the deformed orbital or a spherical proton orbital.

In the present setup, our multilinear model will give up to N choices for the values of the formation amplitude when predicting an unknown case. With commonly accepted tabulations of nuclear deformations and pairing gaps (see, for example, Ref. [24]), it is straightforward to do a systematic calculations on the u and c coefficients for all possible low-lying proton decaying states in nuclei along the proton dripline. The calculations can be done with our codes for deformed shell model and exact pairing diagonalizations that are available to the public [19,25]. We are also developing a simple PYTHON code for that purpose that will be included in the PYTHON package for our multilinear model.

We have focused on the proton decays from nuclei above $Z = 50$ in the analysis above. One may also expect the observation of proton decay from proton-rich nuclei below that shell closure, which can be important not only for nuclear structure but also for the astrophysical rapid-proton capture (rp) process. There have been quite many β delayed proton emissions observed in the light nuclei (see Table 1 in Ref. [14]

TABLE I. Experimentally observed proton decays from nuclei below $Z = 50$, the extract proton decay amplitudes and their values in pdu as well as the orbital angular momentum l , radius parameter ρ' and the classifier k of the $N = 3$ model.

Nucleus	$T_{1/2}^p$	$\log_{10} RF_l(R) ^2$	$RF_l(R)$ (pdu)	l	ρ'	k
^{93}Ag	228(16) ns	-1.750	0.196	4	15.8	2
^{72}Rb	103(22) ns	-1.900	0.192	3	13.5	2
^{54m}Ni	0.73(6) μs	-6.804	7.78×10^{-6}	7	11.2	1
^{53m}Co	18.8(6) s	-7.515	1.78×10^{-8}	9	11.0	1

and the compilation of Ref. [26]). But the observation of direct proton emission was for long time limited to the isomeric state in ^{53m}Co [27,28] (which was the first observed proton decay case) and was recently extended to ^{54m}Ni [29]. Direct ground state decays have been observed from the nucleus ^{72}Rb [30] and ^{93}Ag [31]. The Q values for nuclei including $^{28,30}\text{Cl}$ [32], ^{66}As , ^{73}Rb [30,33], and ^{89}Rh [31] are also measured. But their decay half-lives are not known yet. In Table I we have listed the available proton decay observations. The extracted proton decay probabilities for ^{93}Ag and ^{72}Rb agree well with classification $k = 2$ in our simple $N = 3$ model in relation to the fact that the decaying orbital indeed corresponds to the expected dominant components ($g_{9/2}$ and $f_{5/2}$) in their ground state wave functions. The decays of ^{53m}Co and ^{54m}Ni are highly hindered with $k = 1$ since one would only expect a tiny occupation of the $l = 9, 7$ orbitals in those isomeric states. The fine structure for the proton decays of ^{53m}Co and ^{54m}Ni have also been observed [28,29] which, as expected, also show strong hindrance but less than those decays to the ground states.

IV. SUMMARY

In summary, we have shown in this paper that the proton formation probabilities, extracted from experimental decay half-lives and Q values, can be well represented by a simple multilinear formula with only three parameters, Eq. (3). To determine the model parameter, we applied the usual root

mean square deviation method as well as the mini-max and Bayesian analysis approaches by considering the fact that the total number of proton decay data points are still relatively low. The results obtain from above three approaches are very similar to each other which indicates that the model is quite robust. In particular, the recent experimental data agree very well with the model predictions from all above three approaches. Based on the variance and Bayesian analysis of the multilinear model, we have studied the theoretical uncertainties of the parameters and the model predictions. In addition to the well reproduction of the systematic trends, the multilinearity of the model also provide a way to classify the relative hindrance of different proton decays. It can also be compared with theoretical calculations on the formation probability and similar quantities like the spectroscopic factor.

We deem the presence of a classifier as a useful feature of the model. But one possible disadvantage of the model is that it will not predict a unique value for a new or unknown proton decay data but a set of classifiers instead. Here, we would like to emphasize that an extremely good agreement between experimental data and the multilinear fit can be achieved already with $N = 3$ which divides the available experimental data into three groups from the most hindered (due to large deformation or pairing hindrance), intermediate as well as most favored (single-particle state) decays. That could provide much more useful nuclear structure information than the absolute value of the formation probability from a systematic perspective. When predicting unknown proton decays, the choices of classifier value k can be further constrained by simple deformed shell model plus exact pairing calculations that will be included in the PYTHON package to be distributed for the present multilinear model.

ACKNOWLEDGMENTS

C.Q. acknowledges the computational support provided by the National Academic Infrastructure for Supercomputing in Sweden (NAISS) at PDC, KTH, and support from the Olle Engkvist's Foundation. We thank K. Sallmén for discussions on the Bayesian analysis and Gaussian process and W. Zhang for sharing with us his latest experimental data.

-
- [1] K. Auranen *et al.*, *Phys. Lett. B* **792**, 187 (2019).
[2] W. Zhang *et al.*, *Commun. Phys.* **5**, 285 (2022).
[3] K. Auranen *et al.*, *Phys. Rev. Lett.* **128**, 112501 (2022).
[4] F. Wang *et al.*, *Phys. Lett. B* **770**, 83 (2017).
[5] D. T. Doherty *et al.*, *Phys. Rev. Lett.* **127**, 202501 (2021).
[6] H. Geiger and J. M. Nuttall, *Philos. Mag.* **22**, 613 (1911); H. Geiger, *Z. Phys.* **8**, 45 (1922).
[7] D. S. Delion, *Theory of Particle and Cluster Emission*, Lecture Notes in Physics 819 (Springer, Berlin, 2010).
[8] C. Qi, D. S. Delion, R. J. Liotta, and R. Wyss, *Prog. Part. Nucl. Phys.* **105**, 214 (2019).
[9] D. S. Delion, R. J. Liotta, and R. Wyss, *Phys. Rev. Lett.* **96**, 072501 (2006).
[10] D. S. Delion, R. J. Liotta, and R. Wyss, *Phys. Rep.* **424**, 113 (2006).
[11] C. Qi, D. S. Delion, R. J. Liotta, and R. Wyss, *Phys. Rev. C* **85**, 011303(R) (2012).
[12] D. S. Delion and A. Dumitrescu, *Phys. Rev. C* **103**, 054325 (2021).
[13] C. Qi, R. Liotta, and R. Wyss, *Phys. Lett. B* **818**, 136373 (2021).
[14] B. Blank and M. J. G. Borge, *Prog. Part. Nucl. Phys.* **60**, 403 (2008).
[15] M. Pfützner, M. Karny, L. V. Grigorenko, and K. Riisager, *Rev. Mod. Phys.* **84**, 567 (2012).
[16] See Supplemental Material at <http://link.aps.org/supplemental/10.1103/PhysRevC.108.054311> for more results from the

- fitting and the detailed analysis on the proton decay formation amplitudes in particle decay unit (pdu).
- [17] G. F. Bertsch, B. Sabbey, and M. Uusnakki, *Phys. Rev. C* **71**, 054311 (2005).
- [18] C. Qi, *J. Phys. G: Nucl. Part. Phys.* **42**, 045104 (2015).
- [19] Z. Y. Wu, C. Qi, R. Wyss, and H. L. Liu, *Phys. Rev. C* **92**, 024306 (2015).
- [20] D. R. Phillips, R. J. Furnstahl, U. Heinz, T. Maiti, W. Nazarewicz, F. M. Nunes, M. Plumlee, M. T. Pratola, S. Pratt, F. G. Viens, and S. M. Wild, *J. Phys. G: Nucl. Part. Phys.* **48**, 072001 (2021).
- [21] A. Boehnlein *et al.*, *Rev. Mod. Phys.* **94**, 031003 (2022).
- [22] C. Qi, F. R. Xu, R. J. Liotta, and R. Wyss, *Phys. Rev. Lett.* **103**, 072501 (2009); C. Qi, F. R. Xu, R. J. Liotta, R. Wyss, C. Asawatangtrakuldee, and D. Hu, *Phys. Rev. C* **80**, 044326 (2009).
- [23] D. Karlsson and C. Qi, NEural Network Regression for alpha particle Formation Amplitude (NERF-A) (unpublished).
- [24] P. Moller, A. J. Sierk, T. Ichikawa, and H. Sagawa, *At. Data Nucl. Data Tables* **109–110**, 1 (2016).
- [25] X. Y. Liu and C. Qi, *Comput. Phys. Commun.* **259**, 107349 (2021).
- [26] F. G. Kondev, M. Wang, W. J. Huang, S. Naimi, and G. Audi, *Chin. Phys. C* **45**, 030001 (2021).
- [27] J. Cerny, J. E. Esterl, R. A. Gough, and R. G. Sextro, *Phys. Lett. B* **33**, 284 (1970).
- [28] L. G. Sarmiento *et al.*, *Nat. Commun.* **14**, 5961 (2023); D. Rudolph, talk at procon2023.
- [29] J. Giovinazzo *et al.*, *Nat. Commun.* **12**, 4805 (2021).
- [30] H. Suzuki *et al.*, *Phys. Rev. Lett.* **119**, 192503 (2017).
- [31] I. Čeliković *et al.*, *Phys. Rev. Lett.* **116**, 162501 (2016).
- [32] I. Mukha *et al.*, *Phys. Rev. C* **98**, 064308 (2018).
- [33] D. E. M. Hoff *et al.*, *Phys. Rev. C* **102**, 045810 (2020).